Original article

MOLECULAR METABOLISM

TIMP3 interplays with apelin to regulate cardiovascular metabolism in hypercholesterolemic mice

Robert Stöhr [1,2,10], Ben Arpad Kappel [1,2,10], Daniela Carnevale [3,4,10], Michele Cavalera [1], Maria Mavilio [1], Ivan Arisi [5], Valentina Fardella [3], Giuseppe Cifelli [3], Viviana Casagrande [1], Stefano Rizza [1], Antonino Cattaneo [6,7], Alessandro Mauriello [8], Rossella Menghini [1], Giuseppe Lembo [3], Massimo Federici [1,9,*]

ABSTRACT

Objective: Tissue inhibitor of metalloproteinase 3 (TIMP3) is an extracellular matrix (ECM) bound protein, which has been shown to be downregulated in human subjects and experimental models with cardiometabolic disorders, including type 2 diabetes mellitus, hypertension and atherosclerosis. The aim of this study was to investigate the effects of TIMP3 on cardiac energy homeostasis during increased metabolic stress conditions.

Methods: ApoE$^{-/-}$TIMP3$^{-/-}$ and ApoE$^{-/-}$ mice on a C57BL/6 background were subjected to telemetric ECG analysis and experimental myocardial infarction as models of cardiac stress induction. We used Western blot, qRT-PCR, histology, metabolomics, RNA-sequencing and in vivo phenotypical analysis to investigate the molecular mechanisms of altered cardiac energy metabolism.

Results: ApoE$^{-/-}$TIMP3$^{-/-}$ revealed decreased lifespan. Telemetric ECG analysis showed increased arrhythmic episodes, and experimental myocardial infarction by left anterior descending artery (LAD) ligation resulted in increased peri-operative mortality together with increased scar formation, ventricular dilatation and a reduction of cardiac function after 4 weeks in the few survivors. Hearts of ApoE$^{-/-}$TIMP3$^{-/-}$ exhibited accumulation of neutral lipids when fed a chow diet, which was exacerbated by a high fat, high cholesterol diet. Metabolomics analysis revealed an increase in circulating markers of oxidative stress with a reduction in long chain fatty acids. Using whole heart mRNA sequencing, we identified apelin as a putative modulator of these metabolic defects. Apelin is a regulator of fatty acid oxidation, and we found a reduction in the levels of enzymes involved in fatty acid oxidation in the left ventricle of ApoE$^{-/-}$TIMP3$^{-/-}$ mice. Injection of apelin restored the hitherto identified metabolic defects of lipid oxidation.

Conclusion: TIMP3 regulates lipid metabolism as well as oxidative stress response via apelin. These findings therefore suggest that TIMP3 maintains metabolic flexibility in the heart, particularly during episodes of increased cardiac stress.

© 2015 The Authors. Published by Elsevier GmbH. This is an open access article under the CC BY-NC-ND license (http://creativecommons.org/licenses/by-nc-nd/4.0/).

Keywords TIMP3; Heart; Lipid metabolism; Apelin; Arrhythmia; Oxidative stress

1. INTRODUCTION

Chronic heart diseases lead to cardiac remodeling, a phenomenon that, besides structural changes, results in an impaired ability of cardiac myocytes to shift between nutrient substrate usage in order to adapt to energetic needs [1]. Several cellular fuel gauges such as AMPK have been found to contribute to the regulation of synchronicity between tissue function and metabolic fluxes in the heart [1]. However, studies from other systems suggest that the extracellular matrix (ECM) may also participate in the regulation of intracellular metabolism [2]. The ECM may be relevant in different chronic heart diseases [3], but how its components interact with intracellular signaling pathways to facilitate dynamic changes in heart metabolism is unknown.

We have recently focused on Tissue inhibitor of Metalloproteinase 3 (TIMP3), an ECM-bound protein, modulating metalloprotease and angiogenic receptors that is downregulated in human subjects and experimental models with metabolic and inflammatory disorders such as type 2 diabetes mellitus, atherosclerosis and heart failure [4–12].

[1]Department of Systems Medicine, University of Rome Tor Vergata, 00133 Rome, Italy [2]Department of Internal Medicine I, University Hospital Aachen, Pauwelsstraße 30, 52074 Aachen, Germany [3]Department of Angiocardioneurology and Translational Medicine, IRCCS Neuromed, 86077 Pozzilli, IS, Italy [4]Department of Molecular Medicine, Sapienza University of Rome, 00161 Rome, Italy [5]Genomics Facility, European Brain Research Institute, Rome, Italy [6]European Brain Research Institute, Rome, Italy [7]Scuola Normale Superiore, Pisa, Italy [8]Department of Biomedicine and Prevention, University of Rome Tor Vergata, 00133 Rome, Italy [9]Center for Atherosclerosis, Department of Medicine, Policlinico Tor Vergata, 00133 Rome, Italy

[10] Robert Stöhr, Ben Arpad Kappel, Daniela Carnevale are equally contributing authors.

*Corresponding author. Department of Systems Medicine, University of Rome "Tor Vergata", Via Montpellier 1, 00133 Rome, Italy. Tel.: +39 06 72596889; fax: +39 06 72596890. E-mail: federicm@uniroma2.it (M. Federici).

Received July 13, 2015 • Revision received July 23, 2015 • Accepted July 27, 2015 • Available online 6 August 2015

http://dx.doi.org/10.1016/j.molmet.2015.07.007

 © 2015 The Authors. Published by Elsevier GmbH. This is an open access article under the CC BY-NC-ND license (http://creativecommons.org/licenses/by-nc-nd/4.0/).

TIMP3 blocks the release of TNF-alpha and EGFR ligands (including TGF-alpha, amphiregulin) mediated by ADAM17. TIMP3 also blocks the activity of metalloproteases such as MMP9 and MMP14, which play a role in progression of heart disease. Finally, TIMP3 blocks the activation of VEGRF2 with a final effect to stabilize the angiogenic process to obtain a mature tube stabilization [13–16].

Previous work showed that loss of TIMP3 accelerates cardiovascular disorders including dilated and hypertrophic cardiomyopathies, abdominal aortic aneurysm and hypertension related vessel remodeling [17,18] mediated by TNF-alpha, Angiotensin II and metalloproteases.

Functional re-expression of TIMP3 via cell-based, vector delivery, or intravenous administration proved a protective role for TIMP3 against complications of myocardial infarction such as cardiac rupture, ischemic related cardiomyopathy and heart fibrosis and pressure overload, suggesting a putative therapeutic role for this protein to preserve tissue integrity, in part via its ability to maintain vasculature structure and mesenchymal stem cell functions [19–21].

The role of TIMP3 in the context of cardiovascular remodeling is relatively unexplored when considering classical risk factors such as hypercholesterolemia, diabetes and hypertension. We have observed that increased levels of TIMP3 released from inflammatory cells partially protect from atherosclerosis progression in a combined genetic and dietetic model, the low density lipoprotein receptor knockout ($LDLR^{-/-}$) mice fed a western diet [10]. Observational studies in subjects with congestive heart failure suggested that TIMP3 might be deficient in the myocardial tissues [22]. We recently described increased atherosclerosis at the aortic level in the $ApoE^{-/-}TIMP3^{-/-}$ mouse model. Here, we demonstrate that $ApoE^{-/-}TIMP3^{-/-}$ mice show decreased lifespan at the baseline and a reduced resistance to cardiac stress. To investigate this phenotype in more depth, we combined genetics, metabolomics and in vivo phenotypical analysis.

Collectively, metabolite profiling and gene and protein expression consistently suggested that the loss of TIMP3 leads to a perturbation of metabolic flexibility in the heart and arrhythmias, phenomena that may underlie the increased rates of cardiovascular death in this model independently from its atherosclerotic background.

2. MATERIALS AND METHODS

2.1. Experimental animal procedures and metabolic tests

All animal procedures were performed in accordance to the Guide for the Care and Use of Laboratory Animals published by the US National Institutes of Health (NIH Publication No. 85–23, revised 1996), approved by the University Hospital of Tor Vergata Animal Care Facility and previously described [23]. $ApoE^{-/-}$ $TIMP3^{-/-}$ mice have previously been described [24]. The genotype was confirmed also assaying TIMP3 protein levels and activity of its substrate Matrix Metalloproteinase 9 (Supplementary Figure S1A-B).

Animals were housed in shoebox-sized cages with free access to water and food on a 12 h day—night cycle. Where specified, animals were fed a Western diet (0.5% cholesterol, 45% calories from fat; Research Diets, New Brunswick, NJ) while all other animals received normal chow food (10% calories from fat; GLP Mucedola Srl, Settimo Milanese, Italy).

Glucose levels were measured in the fasting or fed state as indicated with an OneTouch Lifescan Glucometer. Plasma apelin was measured by ELISA (USCN Lifescience) after overnight fast. All tissues were collected in the fasting or the fed state as indicated and stored at −80. For fasting experiments, animals were fasted for 16 h.

Intraperitoneal glucose tolerance test (IPGTT) was performed after overnight fast. In brief, after a 16 h fast, animals were challenged with glucose (2 g/kg) injected intraperitoneally and blood was collected after 30, 60, 90 and 120 min and analyzed with a glucometer. Intraperitoneal insulin tolerance test (ITT) was performed after a 4 h fast. In brief, animals were challenged with insulin (0.75 U/kg) and blood was collected after 10, 30, 60 and 90 min and analyzed with a glucometer.

2.2. ECG telemetry

ECG recordings were taken in freely moving mice, monitored with a signal transmitter receiver connected to a data acquisition system (Data Sciences International, St Paul, USA.). Data were collected at 1,000 Hz and analyzed with ECG auto software Dataquest Ponemah 4.9 system (Data Sciences International). ECG was continuously recorded for 48 h per mice.

2.3. Acute myocardial infarction model

Ligation of the left anterior descending artery (LAD) was performed as a model of myocardial infarction as previously described [25] and is explained in more detail in the supplementary data.

2.4. Indirect calorimetry

Indirect calorimetry was conducted in $ApoE^{-/-}TIMP3^{-/-}$ mice ($n = 4$) and $ApoE^{-/-}$mice ($n = 4$) as well as in a second experiment after intraperitoneal apelin injections in $ApoE^{-/-}TIMP3^{-/-}$ and $ApoE^{-/-}$ mice ($n = 5$–6 per group). All mice were acclimatized for 24 h to the metabolic cages. O2 consumption (VO2) and CO2 production (VCO2) were measured (TSE Systems, Germany) [26] in mice at 15 min intervals during a 24 h period in the fed state as well as during a 12 h period in the fasting state. Respiratory exchange ratio (RER) (= VCO2/VO2) and lipid oxidation rates {$= [1.672 \times (VO2 - VCO2)]$} were calculated.

2.5. Apelin supplementation

For apelin supplementation studies, Pyr-13 apelin was purchased from DBA Italia and resuspended in PBS. For intraperitoneal injections, a concentration of 0.1 μmol/kg was used as previously described [27]. Control animals received matched volumes of PBS alone.

2.6. Gene expression analysis by qRT-PCR

Total RNA was isolated from liver, heart and muscle using Trizol reagent (Invitrogen Corp, Carlsbad, CA). Two micrograms of total RNA were reverse-transcribed into complementary DNA (cDNA) using the High Capacity cDNA Archive kit (Applied Biosystems, Foster City, CA). Quantitative real-time polymerase chain reaction was performed using an ABI PRISM 7700 System and TaqMan reagents (Applied Biosystems). Each reaction was performed in triplicate using standard reaction conditions and results were normalized by β-actin. Data were submitted to Gene Expression Omnibus (GEO) (GSE53548) [NCBI tracking system #16936641].

2.7. Metabolomics

For Metabolomics analysis, the serum of 6 male $ApoE^{-/-}$ and 6 male $ApoE^{-/-}TIMP3^{-/-}$ was collected in the fasted state. Metabolomics assays were performed in service at Metabolon Laboratory and are described in detail in the supplementary data.

2.8. mRNA profiling and analysis

Total RNA was isolated from hearts of $ApoE^{-/-}$ and $ApoE^{-/-}TIMP3^{-/-}$ mice using Trizol reagent (Invitrogen Corp, Carlsbad, CA). mRNA sequencing was commercially performed at DNAVISION facility (Charleroi, Belgium). RNA libraries were prepared for sequencing using standard Illumina protocols. RNA-Sequencing profiling was performed by the Illumina HiSeq2000 platform. FastQC tool was used for the quality check

 © 2015 The Authors. Published by Elsevier GmbH. This is an open access article under the CC BY-NC-ND license (http://creativecommons.org/licenses/by-nc-nd/4.0/).

of sequenced samples. For data analysis, a pipeline combining TopHat (http://tophat.cbcb.umd.edu) and Cufflinks (http://cuffinks.cbcb.umd.edu) was used to identify transcripts in each sample. TopHat uses the Bowtie aligner to produce alignment and to discover splice junctions. Cufflinks assembles transcripts, estimates their abundances, and tests for differential expression and regulation. Reads were aligned against the mouse reference genome (NCBIM37.60) and the identified transcripts were compared to those annotated in the reference genome. The metric used by Cufflinks to estimate the abundance of transcripts is the FPKM: Fragments Per Kilobase of exon per Million fragments mapped. For heat maps and hierarchical clustering MultiExperiment Viewer was used [28]. Differential exons were computed by EdgeR package in Bioconductor. Data were submitted to GEO (GSE53548) [NCBI tracking system #16936641].

2.9. Statistical analysis

Results of the experimental studies are mean ± SEM. Statistical analyses were performed using the unpaired Student's *t* test and one-way-ANOVA with GraphPAD Prism 6.0 if not otherwise specified. Survival analysis was performed according to the Kaplan Meier method and compared by using the Log-Rank test. Values of $p < 0.05$ were considered statistically significant.

3. RESULTS

3.1. ApoE$^{-/-}$TIMP3$^{-/-}$ mice have increased cardiac mortality

A combined retro- and prospective 52 weeks analysis of ApoE$^{-/-}$TIMP3$^{-/-}$ ($n = 32$) mice revealed a decreased survival rate when compared to ApoE$^{-/-}$ ($n = 32$) littermates ($p = 0.0002$, Cox Test; Figure 1A), with the first episodes of death observed at week 28 in the ApoE$^{-/-}$TIMP3$^{-/-}$ group. The higher mortality rate in the ApoE$^{-/-}$TIMP3$^{-/-}$ group was independent from gender and no differences between genotypes for specific macroscopic signs of infections including dermatitis or sudden loss of body weight were observed. Since necroscopy of ApoE$^{-/-}$TIMP3$^{-/-}$ mice did not reveal any obvious sign such as bleeding, malignancy or macroscopically visible organ pathology responsible for decreased lifespan, we speculated that mice might suffer from sudden cardiac death.

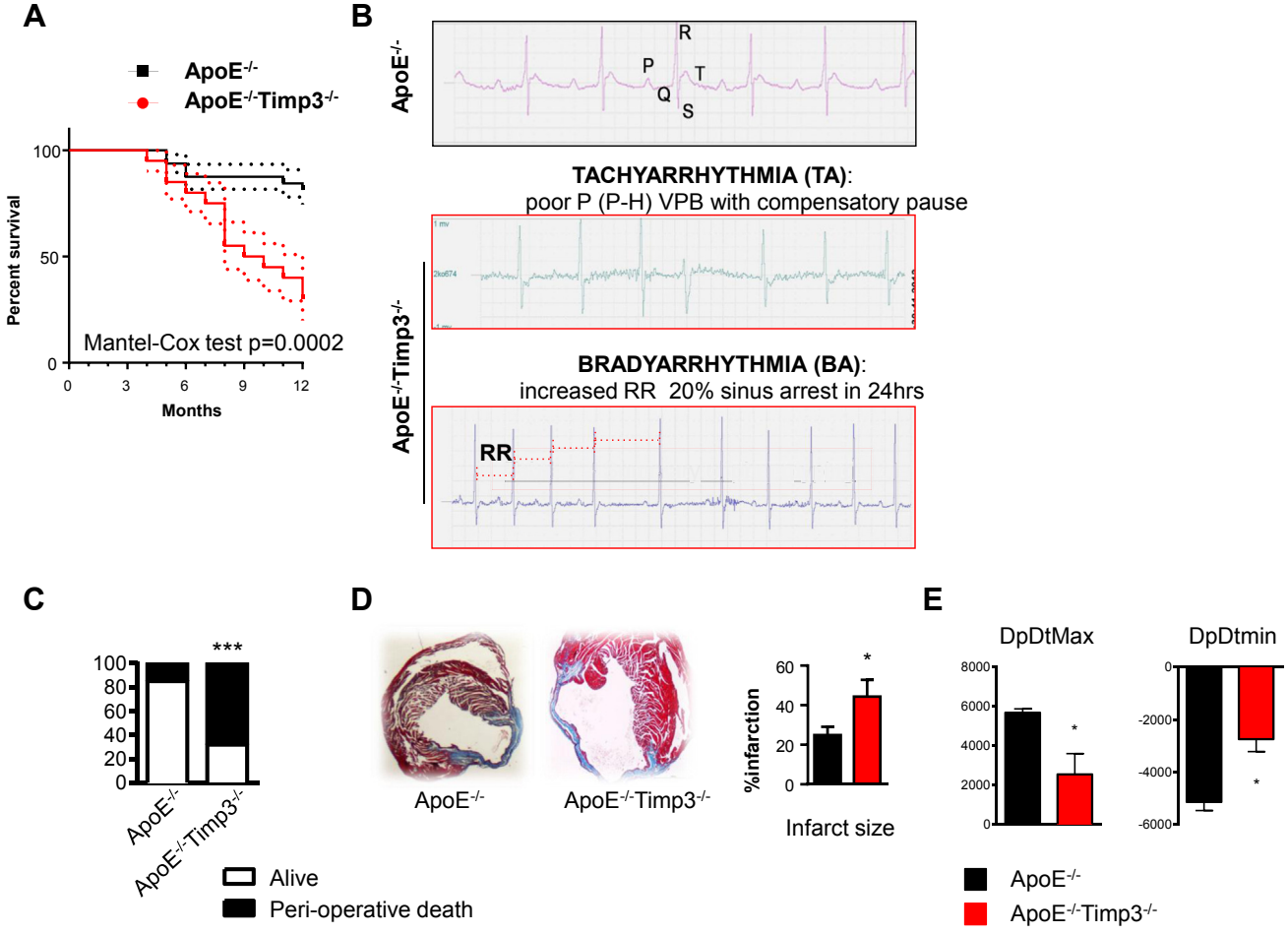

Figure 1: ApoE$^{-/-}$TIMP3$^{-/-}$ animals reveal decreased lifespan, arrhythmias and susceptibility to increased cardiac stress. A) Combined retro- and prospective survival analysis in a cohort of 64 male and female mice ($n = 32$ for ApoE$^{-/-}$TIMP3$^{-/-}$ M/F = 12/20 and $n = 32$ for ApoE$^{-/-}$ M/F = 12/20) over a time period of 12 months ($p = 0.0002$, Cox Test). B) Telemetry 24 h ECG in 32-weeks-old ApoE$^{-/-}$TIMP3$^{-/-}$ and ApoE$^{-/-}$ mice. We observed a higher amount of arrhythmic episodes in ApoE$^{-/-}$TIMP3$^{-/-}$ as well as sudden deaths in 4 out of 6 male mice during the 7-day registration ($p = 0.06$, Fisher's exact test). C) Increased peri-operative mortality during experimental myocardial infarction by LAD ligation in ApoE$^{-/-}$TIMP3$^{-/-}$ (13/19) compared to ApoE$^{-/-}$ (3/13) (***$p < 0.001$ by Chi-square test). D) Representative photomicrographs of Masson-Trichrome stained hearts 4 weeks post-LAD ligation showing increased infarction size as confirmed by morphometric quantification of percent total LV circumference. Data are mean ± SEM (*$p < 0.05$ by Student t-test, $n = 3$–4 per group). E) Reduced systolic (dp/dtmax) and diastolic (dp/dtmin) heart function in ApoE$^{-/-}$TIMP3$^{-/-}$ mice 4 weeks after LAD ligation as measured by Millar Catheter. Data are mean ± SEM (*$p < 0.05$ by Student t-test, $n = 4$–5 per group).

 © 2015 The Authors. Published by Elsevier GmbH. This is an open access article under the CC BY-NC-ND license (http://creativecommons.org/licenses/by-nc-nd/4.0/).

To test this hypothesis of increased cardiac mortality, we subjected ApoE$^{-/-}$TIMP3$^{-/-}$ mice and ApoE$^{-/-}$ littermates to two different models of cardiac stress: invasive telemetry 24 h ECG and LAD ligation. We first performed invasive 24 h ECG recordings to investigate the presence of anomalous electrical activity in 32-weeks-old ApoE$^{-/-}$TIMP3$^{-/-}$ and ApoE$^{-/-}$ mice. We observed a higher amount of arrhythmic episodes in ApoE$^{-/-}$TIMP3$^{-/-}$ mice (Figure 1B) as well as sudden deaths in 4 out of 6 ApoE$^{-/-}$TIMP3$^{-/-}$ male mice during the 7-day registration period ($p = 0.06$, Fisher Exact test).

In the second model of cardiac stress induction, ApoE$^{-/-}$TIMP3$^{-/-}$ and ApoE$^{-/-}$ mice were subjected to LAD ligation as previously described. In the ApoE$^{-/-}$TIMP3$^{-/-}$ cohort, we observed significantly increased peri-operative mortality compared with ApoE$^{-/-}$ mice with 13/19 mice dying within 24 h of the intervention compared to 2/13 deaths in the ApoE$^{-/-}$ group ($p < 0.0001$, Chi-square test, Figure 1C). Although we cannot measure the occurrence of arrhythmias in this experiment, we did not observe bleeding or other operative complications between the 2 groups. In the few survivors, histological analysis of the ventricle showed extension of the infarction area ($p < 0.05$, Student's t-test, $n = 3–4$ per group, Figure 1D) as well as increased ventricular remodeling and dilatation in the ApoE$^{-/-}$TIMP3$^{-/-}$ mice (Figure 1D). Invasive cardiac function 4 weeks post LAD ligation revealed reduced systolic and diastolic function in ApoE$^{-/-}$TIMP3$^{-/}$ mice ($p < 0.05$ for both, Student's t-test, Figure 1E).

3.2. ApoE$^{-/-}$TIMP3$^{-/-}$ mice show lipid accumulation in heart

To gain further insight into structural changes within the heart of ApoE$^{-/-}$TIMP3$^{-/-}$ mice leading to arrhythmias and sudden cardiac death, we performed echocardiographic and histological analyses.

As expected ApoE$^{-/-}$TIMP3$^{-/-}$ mice revealed signs of mild atherosclerosis in both coronary and carotid arteries but no signs of atherothrombosis (Supplementary Figure S2A–B). Left ventricular function as measured with echocardiography did not differ between the groups (Supplementary Figure S2C).

However, staining of heart sections with Oil Red O revealed focal intracellular accumulation of lipid droplets in the hearts of the ApoE$^{-/-}$TIMP3$^{-/-}$ mice, a phenomenon absent in ApoE$^{-/-}$ mice fed a normal diet at 24 weeks of age (Figure 2A). When both mouse strains were fed a Western diet for 8 weeks we observed intense and significant higher lipid accumulation in the ApoE$^{-/-}$TIMP3$^{-/-}$ group compared with ApoE$^{-/-}$ mice ($p < 0.05$, Student's t-test, Figure 2B).

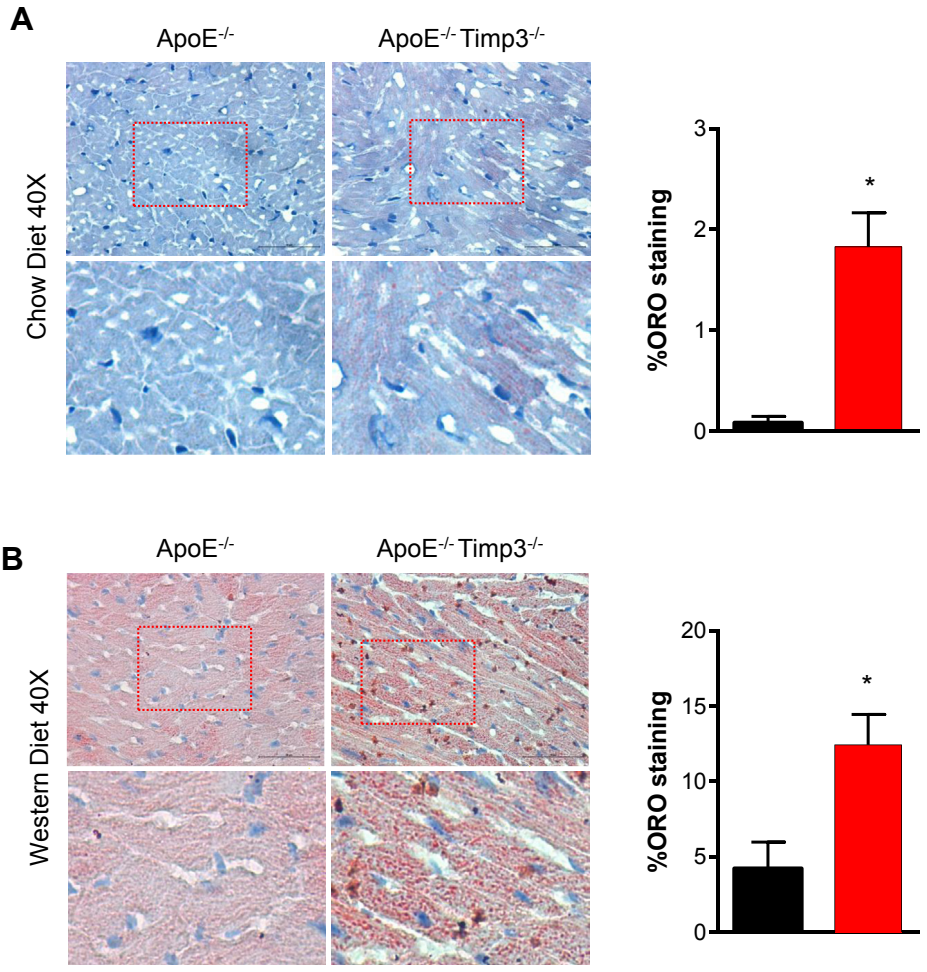

Figure 2: ApoE$^{-/-}$TIMP3$^{-/-}$ animals show increased deposition of neutral lipids in the heart on normal chow and western diet. A) Representative sections of myocardium of 6–8 month old ApoE$^{-/-}$TIMP3$^{-/-}$ and ApoE$^{-/-}$ mice on normal chow diet stained with ORO. B) Representative sections and quantification of myocardium from 6 to 8 month old mice fed a Western diet for 8 weeks stained with ORO showing increased lipid deposition in hearts of ApoE$^{-/-}$TIMP3$^{-/-}$ mice. Data are mean ± SEM (*$p < 0.05$, Student t-test, $n = 4$ per group). Magnification further displays globular intracellular lipid accumulation and a punctate pattern reminiscent of extracellular lipid deposition in ApoE$^{-/-}$TIMP3$^{-/-}$ animals.

 © 2015 The Authors. Published by Elsevier GmbH. This is an open access article under the CC BY-NC-ND license (http://creativecommons.org/licenses/by-nc-nd/4.0/).

3.3. Metabolic characterization of ApoE$^{-/-}$TIMP3$^{-/-}$ mice reveals impaired lipid oxidation

ApoE$^{-/-}$TIMP3$^{-/-}$ mice further showed a complex metabolic phenotype characterized by a trend to lower fasting glucose, a normal Glucose Tolerance Test (GTT) coupled to mild insulin resistance during the Insulin Tolerance Test (*$p < 0.05$, ***$p < 0.001$, Student's t test, Figure 3A–C).

Whole-body indirect calorimetry of ApoE$^{-/-}$TIMP3$^{-/-}$ compared to ApoE$^{-/-}$ mice revealed no difference in the fed state (data not shown). However, because the observed differences in the fasting glucose, we repeated the whole-body indirect calorimetry during 12 consecutive hours of fasting conditions. While no differences were observed in the 0–8 h interval (data not shown), we observed that in the interval from 8 to 12 h of fasting the RER was significantly increased due to significantly reduced lipid oxidation (both $p < 0.05$, Student's t test, Figure 3D).

3.4. Metabolomics analysis revealed changes in biomarkers of antioxidant defense, lipid metabolism and sphingolipid pathway

To unveil biomarkers associated to the reduced lifespan and impaired lipid oxidation, we performed metabolomics analysis in ApoE$^{-/-}$ and ApoE$^{-/-}$TIMP3$^{-/-}$. Random Forest analysis of the analyzed biochemicals resulted in a predictive accuracy of 83% in classifying between ApoE$^{-/-}$ and ApoE$^{-/-}$TIMP3$^{-/-}$ mice (Supplementary Figure S3). Several metabolites were differently regulated in the ApoE$^{-/-}$TIMP3$^{-/-}$ compared with ApoE$^{-/-}$ littermates (Supplementary Tables S1 and S2). In the serum of ApoE$^{-/-}$TIMP3$^{-/-}$ mice, we observed complex modulation of pathways linked to oxidative stress as demonstrated by the depletion of ergothioneine, equol sulfate, cysteine-glutathione disulfide and oxidized glutathione while 2-hydroxybutyrate and 2-aminobutyrate were increased (Figure 4A,B). ApoE$^{-/-}$TIMP3$^{-/-}$ mice also showed reductions in long-chain monounsaturated FFAs such as 10-nonadecenoate and 10-heptadecenoate, medium-chain acyl-carnitines such as hexanoylcarnitine, medium-chain acyl-glycine (i.e., valerylglycine) and the medium-chain fatty acid marker of beta-oxidation, 3-hydroxydecanoate (Figure 5A,B). On the other hand, the long-chain acyl-carnitine stearoylcarnitine was significantly elevated in ApoE$^{-/-}$TIMP3$^{-/-}$ mice (Figure 5A,B). ApoE$^{-/-}$TIMP3$^{-/-}$ mice also showed altered sphingolipid metabolism with increased levels of palmitoyl sphingomyelin, stearoyl sphingomyelin, 1-stearoylglycerol and sphingosin that can be in part connected to increased stearoylcarnitine and its derivatives (Figure 6A,B).

3.5. Reduced expression of enzymes involved in fatty acid oxidation in ApoE$^{-/-}$TIMP3$^{-/-}$ mice

The relative deficiency of long-chain fatty acids along with the concomitant build-up of stearoylcarnitine could reflect a deficiency in stearoyl-CoA desaturase 1 (SCD1) within different tissues. We therefore screened the expression of genes related to the regulation of glucose and lipid metabolism in ApoE$^{-/-}$TIMP3$^{-/-}$ compared with ApoE$^{-/-}$ mice in the liver, skeletal muscle and heart. In the liver, we found reduced mRNA expression for PPARα, SCD1, ACADM, ACADL, ACADVL

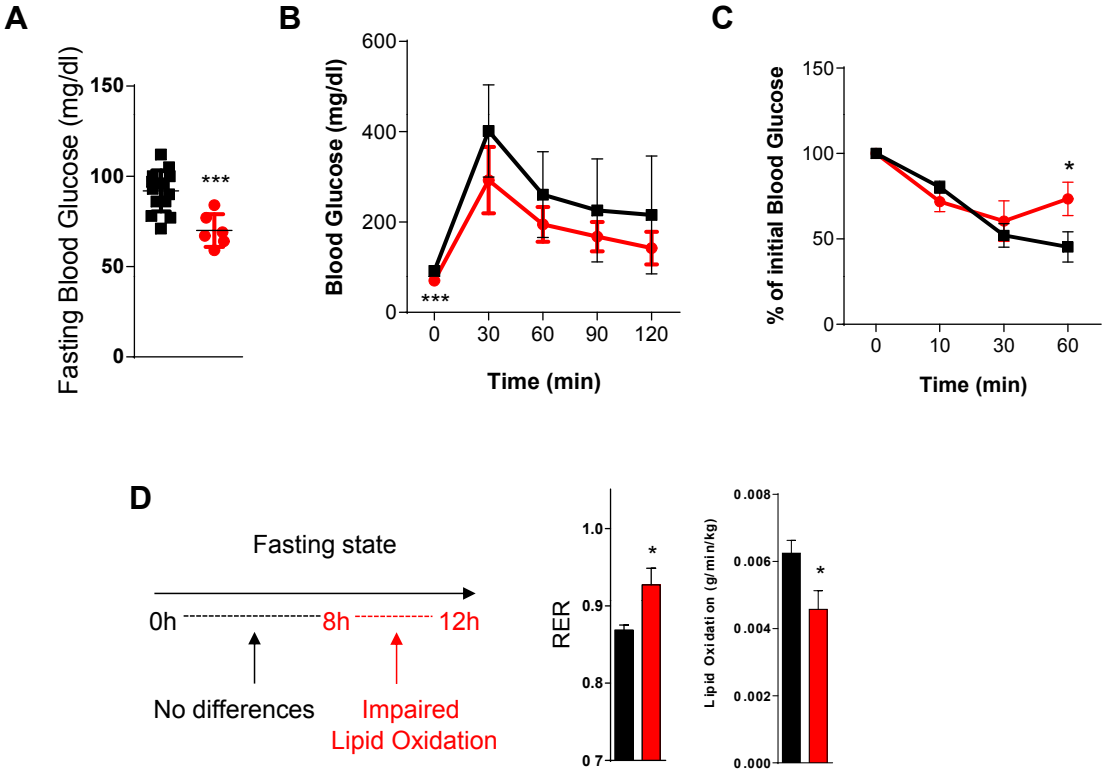

Figure 3: Metabolic characterization of ApoE$^{-/-}$TIMP3$^{-/-}$ mice reveals impaired lipid oxidation. A) Analysis of fasting glucose levels reveals significant reduction in ApoE$^{-/-}$TIMP3$^{-/-}$ mice (***$p < 0.001$, Student's t test, n = 14 for ApoE$^{-/-}$ and n = 6 for ApoE$^{-/-}$TIMP3$^{-/-}$ per group). B) Intraperitoneal Glucose Tolerance test shows no significant differences between the two groups (n = 14 for ApoE$^{-/-}$ and n = 6 for ApoE$^{-/-}$TIMP3$^{-/-}$ per group). C) Mild insulin resistance of ApoE$^{-/-}$TIMP3$^{-/-}$ mice at the Insulin Tolerance Test (*$p < 0.05$, Student's t test, n = n = 4 for ApoE$^{-/-}$ and n = 5 for ApoE$^{-/-}$TIMP3$^{-/-}$ per group). D) Indirect calorimetry of ApoE$^{-/-}$TIMP3$^{-/-}$ compared to ApoE$^{-/-}$ mice during 12 consecutive hours of fasting conditions. Data show the interval from 8 to 12 h of fasting. RER was significantly increased and lipid oxidation significantly reduced in ApoE$^{-/-}$TIMP3$^{-/-}$ mice (*$p < 0.05$, Student's t test, n = 3–4).

 © 2015 The Authors. Published by Elsevier GmbH. This is an open access article under the CC BY-NC-ND license (http://creativecommons.org/licenses/by-nc-nd/4.0/).

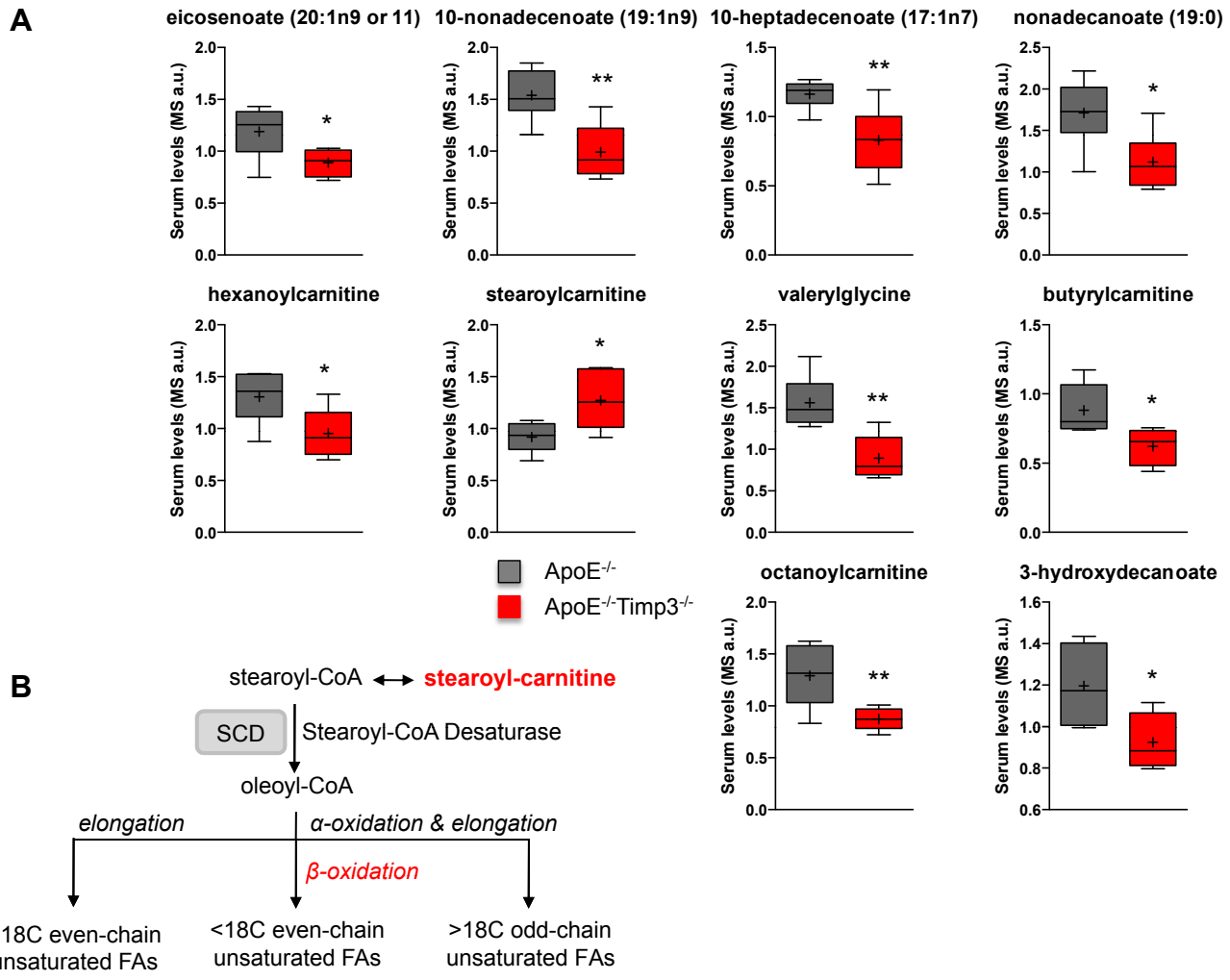

Figure 4: ApoE$^{-/-}$TIMP3$^{-/-}$ mice have impairment of fatty acid metabolism. A) Metabolomics analysis of the serum shows a decrease in long-chain monounsaturated FFAs, medium-chain acyl-carnitines and medium-chain fatty acid markers in ApoE$^{-/-}$TIMP3$^{-/-}$ animals (*p $\leq$ 0.05 and **p $<$ 0.01, Student's t test, n = 6 per group). B) Regulation of MUFA/SUFA balance in mammalian cell lipids by SCD1.

and FoxO1 (Supplementary Table S3). In skeletal muscle, no important differences were found (Supplementary Table S3). In the hearts of ApoE$^{-/-}$TIMP3$^{-/-}$ mice, we found significantly decreased expression of PPARα and its targets SCD1, ACADM and a trend for decreased expression of other enzymes involved in fatty acid oxidation such as ACADL and ACADVL (Table 1). Interestingly, we also found decreased expression of FoxO1, a regulator of oxidative stress and autophagy, and its targets PDK4, ATG5, ATG8, BECN1, LC3, ULK1 (Table 1).

3.6. Whole heart mRNA sequencing revealed reduced apelin in ApoE$^{-/-}$TIMP3$^{-/-}$ mice

To gain insight into the regulation of glucose and lipid metabolism of the heart by TIMP3 we performed mRNA transcriptomic analysis by Next Generation Sequencing (Illumina) of the heart in ApoE$^{-/-}$TIMP3$^{-/-}$ and ApoE$^{-/-}$ littermates. We identified several significantly upregulated and downregulated transcripts from ApoE$^{-/-}$TIMP3$^{-/-}$ compared with ApoE$^{-/-}$ littermates (Supplementary Figure S4A and Supplementary Table S4). Among the downregulated transcripts, confirmed after qPCR, we found apelin (Supplementary Figure S4A,B), which we confirmed to be significantly reduced in heart tissue but not in the epididymal White Adipose Tissue (eWAT), muscle and liver from ApoE$^{-/-}$ TIMP3$^{-/-}$ mice by quantitative PCR (*p $<$ 0.05, Student's t test, Figure 7A). Apelin blood levels measured by ELISA were shown to be significantly lower in the ApoE$^{-/-}$TIMP3$^{-/-}$ compared with ApoE$^{-/-}$ littermates (*p $<$ 0.05, Student's t test, Figure 7B).

3.7. Apelin injection rescues metabolic phenotype in ApoE$^{-/-}$TIMP3$^{-/-}$ mice

Finally, we reasoned that injecting apelin in vivo could lead to improvement of metabolic defects observed in ApoE$^{-/-}$TIMP3$^{-/-}$ mice. Indirect calorimetry was performed in fasted ApoE$^{-/-}$TIMP3$^{-/-}$ mice and ApoE$^{-/-}$ littermates after a single intraperitoneal apelin injection; control animals received a matched volume of PBS (per group n = 5–6; values reported in the bar graph were obtained in the interval of prolonged fasting (8–12 h interval)). Apelin injection significantly reduced RER in ApoE$^{-/-}$TIMP3$^{-/-}$ mice (****p $<$ 0.001, one-way ANOVA, Figure 7C) to an extent comparable to PBS-injected ApoE$^{-/-}$ littermates. RER: 0.80 $\pm$ 0.02 (ApoE$^{-/-}$ PBS) vs. 0.79 $\pm$ 0.02 (ApoE$^{-/-}$ TIMP3$^{-/-}$ apelin), not significant, Figure 7C). Consequently, apelin increased lipid oxidation in ApoE$^{-/-}$TIMP3$^{-/-}$ mice and in ApoE$^{-/-}$ mice, although to a lesser extent (****p $<$ 0.001, one-way ANOVA, Figure 7C).

 © 2015 The Authors. Published by Elsevier GmbH. This is an open access article under the CC BY-NC-ND license (http://creativecommons.org/licenses/by-nc-nd/4.0/).

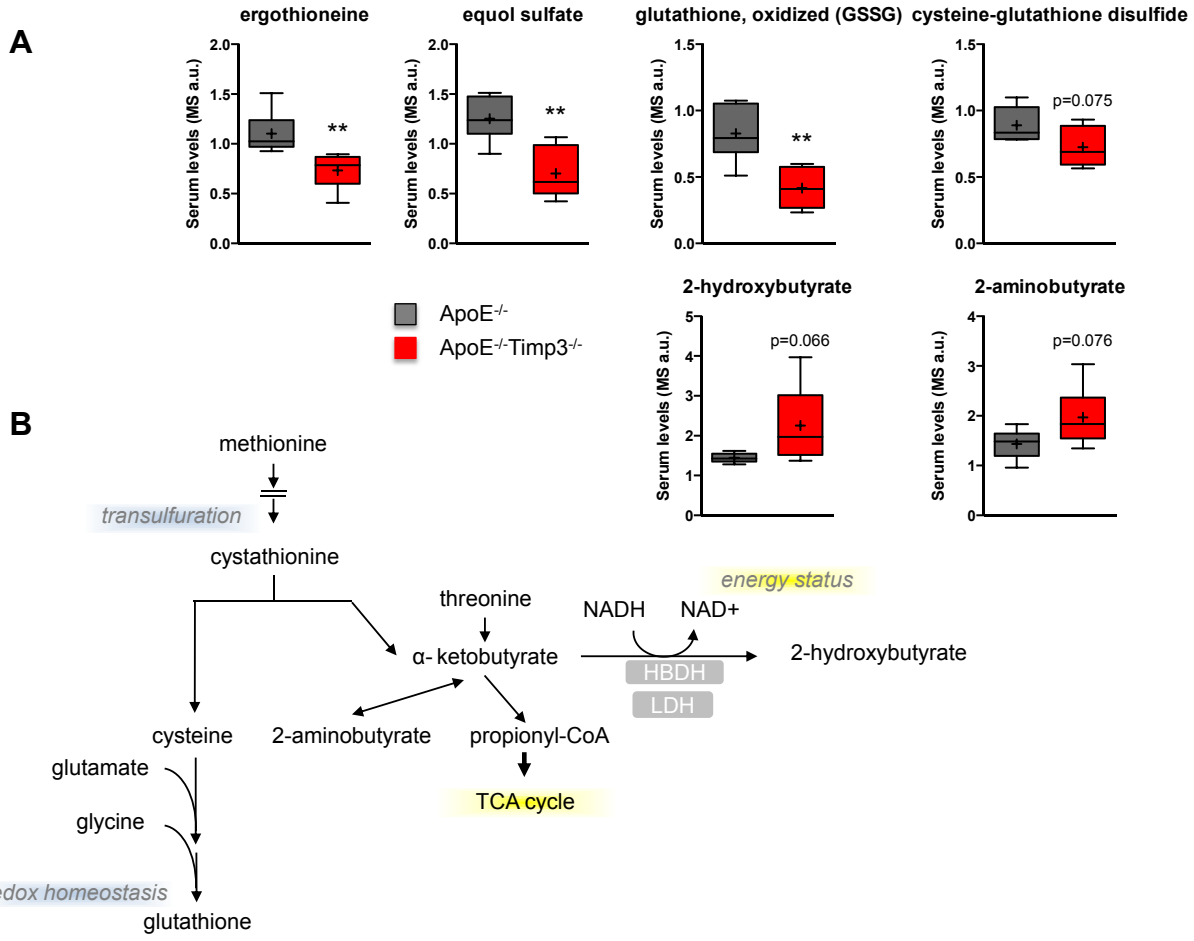

Figure 5: ApoE$^{-/-}$TIMP3$^{-/-}$ mice have loss of defense against oxidative stress. A) Metabolomics analysis of the serum of ApoE$^{-/-}$TIMP3$^{-/-}$ vs. ApoE$^{-/-}$ animals shows a depletion of dietary antioxidants suggesting a loss of dietary antioxidant and anti-inflammatory chemicals (*p $\leq$ 0.05, **p $<$ 0.01 and ***p $<$ 0.001, Student's t test, n $=$ 6 per group). B) Glutathione regulation pathway in mammalian cells.

4. DISCUSSION

The phenotype of the ApoE$^{-/-}$TIMP3$^{-/-}$ mice revealed new, unpredicted findings linking TIMP3 to metabolic flexibility in the heart. Although, compared to control ApoE$^{-/-}$ littermates, the ApoE$^{-/-}$TIMP3$^{-/-}$ mice showed mild increased atherosclerotic plaques and fatty streaks at the aortic roots and the peripheral aorta, the differences were less consistent in the coronary and carotid arteries. It is possible, therefore, that the causes of sudden death are not linked to plaque instability and a possible metabolic origin of the phenotype cannot be excluded. Previous work on the combined ApoE and high-density lipoprotein receptor SR-BI (SR-BI) double knockout revealed early lethality due to increased coronary atherosclerosis combined with lipid accumulation in the left ventricle [29]. The ApoE$^{-/-}$TIMP3$^{-/-}$ mice showed similar globular intracellular lipid accumulation, and when shifted to Western diet, a punctate pattern reminiscent of extracellular lipid deposition [29].

However, differently from the ApoE$^{-/-}$SR-BI$^{-/-}$ model, the ApoE$^{-/-}$TIMP3$^{-/-}$ mice revealed increased lethality at an older age or when subjected to stress conditions like telemetry or experimental myocardial infarction, suggesting that the effect may be partially age- and environment dependent, as already observed with TIMP3 in other cardiovascular models [15,16].

Metabolomics data allows for a hypothesis that explains the increased susceptibility of ApoE$^{-/-}$TIMP3$^{-/-}$ mice to cardiovascular diseases. First, ApoE$^{-/-}$TIMP3$^{-/-}$ mice have defective control of oxidative stress. In particular, they show a state of depletion of dietary antioxidants such as ergothioneine and equol sulfate [30, 31] coupled to the decrease of some indicators of oxidation such as cysteine-glutathione disulfide and oxidized glutathione. Similarly, we found increased concentrations of 2-hydroxybutyrate and 2-aminobutyrate, both being derived from the common precursor alpha-ketobutyrate, the levels of which increase when demand for glutathione is high. Since it has been reported that ischemia induces glutathione depletion via osmotic stress [32], it is intriguing to hypothesize that TIMP3 deficiency in the heart mimics the effect of modified lipoproteins and oxysterols to provoke an ischemia-like metabolic alterations at the myocardial level although we cannot exclude the involvement of other tissues [33,34].

Secondly, analysis of sphingolipid metabolism displayed deep perturbations in ApoE$^{-/-}$TIMP3$^{-/-}$ mice. Glutathione depletion has been shown to regulate sphingomyelin metabolism [35], and the loss of an oxidative stress response might be responsible for those alterations. In patients with transient ischemia, and thus increased cardiac stress, increased levels of sphingosine have been found [36]. Further, alterations of sphingolipid metabolism have been reported in rats subjected to LAD ligation [37] and in models of ischemia/reperfusion injury [38,39].

Although, we could not identify ceramide itself in the metabolomics analysis, it is a crucial intermediate of sphingolipid metabolism

 © 2015 The Authors. Published by Elsevier GmbH. This is an open access article under the CC BY-NC-ND license (http://creativecommons.org/licenses/by-nc-nd/4.0/).

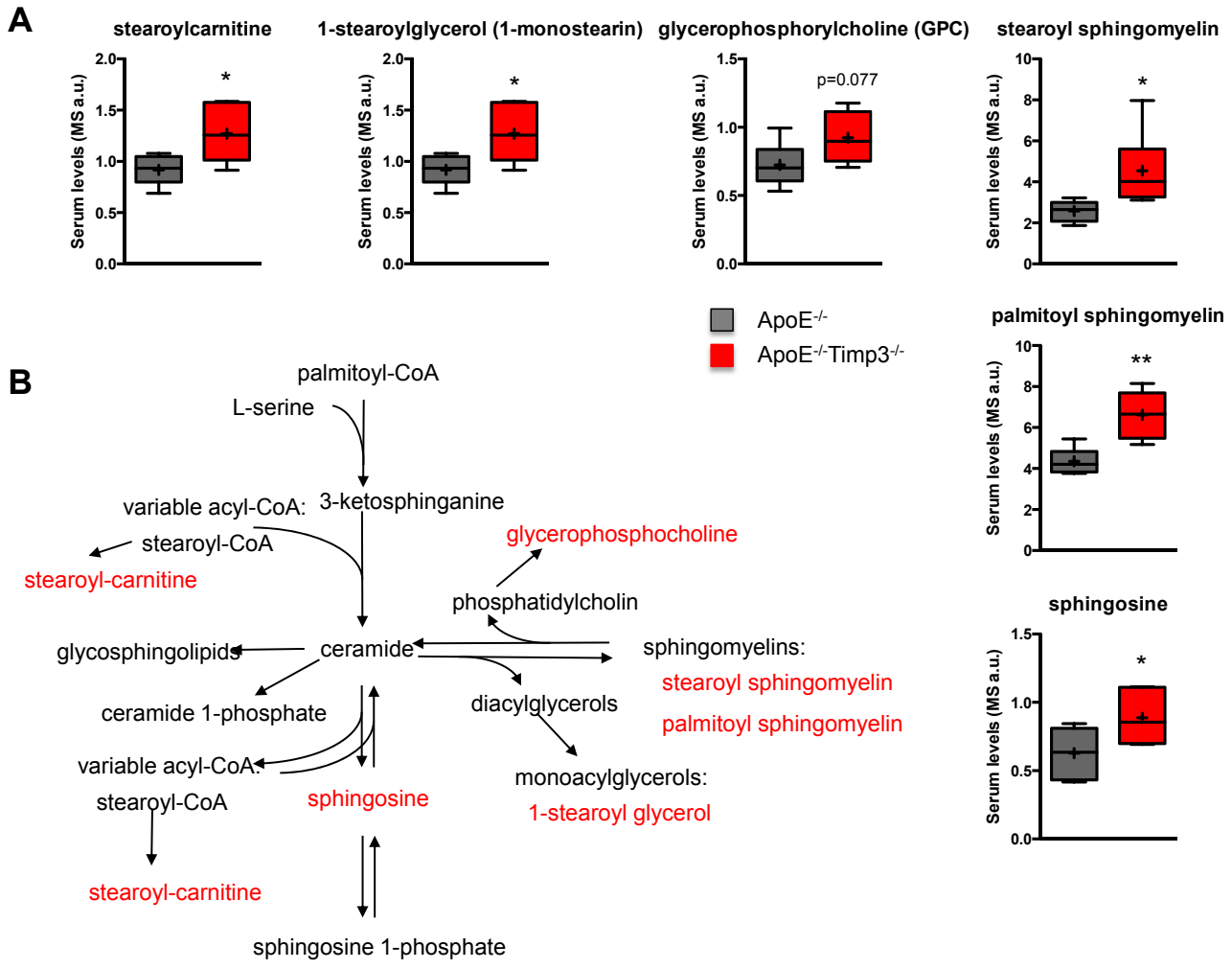

Figure 6: ApoE$^{-/-}$TIMP3$^{-/-}$ mice have disturbed sphingolipid metabolism. A) Altered sphingolipid metabolism in ApoE$^{-/-}$TIMP3$^{-/-}$ mice revealed by metabolomics analysis of the serum (*$p \leq 0.05$, **$p < 0.01$ and ***$p < 0.001$, Student's t test, $n = 6$ per group). B) Sphingolipid metabolism in mammalian cells that can be in part connected to increased stearoylcarnitine and its derivatives.

(Figure 6B) and has been associated with the dysfunction of the human ether-a-go-go related gene (HERG) K+ channel, which, again, is associated with prolongation of the QT interval and arrhythmias [40]. Therefore, perturbations in sphingolipid metabolism might contribute in increased arrhythmias in the ApoE$^{-/-}$TIMP3$^{-/-}$ mice.

Thirdly, the circulating metabolite profiles suggest that in the face of mild insulin resistance, the loss of TIMP3 in the hypercholesterolemic background is characterized by a block of fatty acid oxidation at the stearoyl-CoA level. This may prompt increased rates of glucose oxidation to support energetic demands. Mice with stearoyl-CoA desaturase 1 deficiency reveal a similar phenotype to ApoE$^{-/-}$TIMP3$^{-/-}$ mice, with increased myocardial glucose utilization and impaired fatty acid oxidation [41]. The limited gene expression screening that we performed in the liver and the muscle confirmed that in this specific context the defective fatty acid oxidation is more prevalent at the cardiovascular level. Therefore, in a TIMP3 deficient state it appears that the heart may be less efficient at compensating for energetic demands during acute stress.

Adult cardiomyocytes produce most energy via fatty acid oxidation (FAO) but retain capacity to readily switch to glucose or other substrate utilization when fatty acid is not available or FAO is compromised [1]. Indeed, when subjecting the myocardium to acute oxidative stress and energy depletion in the model of myocardial infarction, there is an increased mortality, which could be explained by an inability to utilize all metabolic pathways available to produce energy. One may postulate that the lower fasting glucose observed in the ApoE$^{-/-}$TIMP3$^{-/-}$ mice results from a switch to glucose oxidation that impairs a further increase energy production thus ultimately leading to cell death. The reduction PPARα and some of its target genes involved in fatty acid oxidation (such as Hadha Hadhb ACADS ACADM ACADVL) might in part explain the phenotype of the ApoE$^{-/-}$TIMP3$^{-/-}$ mice. In fact, myocardial lipid accumulation and hypoglycemia also characterize the adult mice lacking PPARα [42]. Similarly to the ApoE$^{-/-}$TIMP3$^{-/-}$, deletion of PPARα results in decreased expression of fatty acid β-oxidation genes accompanied by a decrease in fatty acid β-oxidation and a parallel increase in glucose oxidation [42–46]. The ApoE$^{-/-}$TIMP3$^{-/-}$ model may also recall the phenotype characterizing a model of cardiovascular insulin resistance, the Cardiac Insulin Receptor Knockout (CIRKO) mice, in which PPARα and several FAO genes are repressed [47]. Further, we observed a downregulation of

 © 2015 The Authors. Published by Elsevier GmbH. This is an open access article under the CC BY-NC-ND license (http://creativecommons.org/licenses/by-nc-nd/4.0/).

Table 1 — Loss of TIMP3 leads to altered expression of genes involved in fatty acid metabolism in heart.

Heart	Fasting			Fed		
	ApoE$^{-/-}$	ApoE$^{-/-}$ TIMP3$^{-/-}$	p value	ApoE$^{-/-}$	ApoE$^{-/-}$ TIMP3$^{-/-}$	p value
PPARα	**0.72 ± 0.15**	**0.36 ± 0.02**	**0.04**	0.46 ± 0.04	0.47 ± 0.06	0.82
PPARβ	0.74 ± 0.07	0.74 ± 0.07	0.95	0.45 ± 0.03	0.44 ± 0.03	0.84
PPARγ	0.85 ± 0.12	0.79 ± 0.097	0.70	0.26 ± 0.03	0.28 ± 0.04	0.81
FoxO1	**1.27 ± 0.38**	**0.45 ± 0.03**	**0.0495**	**1.05 ± 0.12**	**0.55 ± 0.10**	**0.03**
ERRα	1.92 ± 0.40	1.41 ± 0.22	0.30	0.97 ± 0.12	1.15 ± 0.19	0.44
LXRα	0.96 ± 0.06	0.91 ± 0.08	0.68	**0.39 ± 0.02**	**0.47 ± 0.03**	**0.03**
LXRβ	0.79 ± 0.11	0.64 ± 0.11	0.38	0.43 ± 0.06	0.33 ± 0.03	0.28
Ehhadh	*0.57 ± 0.15*	*0.25 ± 0.03*	*0.08*	0.06 ± 0.01	0.09 ± 0.02	0.12
Hadha	*1.02 ± 0.11*	*0.80 ± 0.05*	*0.09*	0.39 ± 0.02	0.45 ± 0.04	0.27
Hadhb	0.68 ± 0.09	0.62 ± 0.09	0.63	0.36 ± 0.02	0.40 ± 0.06	0.54
ACADS	1.29 ± 0.16	1.34 ± 0.19	0.84	0.83 ± 0.14	0.82 ± 0.14	0.98
ACADM	**1.29 ± 0.15**	**0.79 ± 0.13**	**0.047**	0.60 ± 0.05	0.69 ± 0.11	0.43
ACADVL	*1.21 ± 0.12*	*0.90 ± 0.05*	*0.07*	0.60 ± 0.10	0.55 ± 0.06	0.76
ACADL	1.08 ± 0.06	0.97 ± 0.01	0.12	0.57 ± 0.07	0.57 ± 0.07	0.94
CPT1α	1.10 ± 0.11	1.12 ± 0.08	0.89	*0.34 ± 0.02*	*0.50 ± 0.07*	*0.09*
PDK4	**1.14 ± 0.08**	**0.78 ± 0.10**	**0.03**	**0.03 ± 0.01**	**0.07 ± 0.02**	**0.048**
SCD1	**0.94 ± 0.04**	**0.71 ± 0.07**	**0.02**	0.49 ± 0.08	0.52 ± 0.06	0.78
PGC1α	0.57 ± 0.12	0.56 ± 0.08	0.98	0.25 ± 0.02	0.32 ± 0.07	0.29
PGC1β	1.41 ± 0.24	1.44 ± 0.25	0.93	1.01 ± 0.20	1.24 ± 0.14	0.41
GLUT4	1.48 ± 0.24	1.54 ± 0.22	0.85	1.25 ± 0.29	1.17 ± 0.12	0.80
ATG5	0.82 ± 0.08	0.72 ± 0.04	0.30	0.76 ± 0.12	0.73 ± 0.17	0.86
ATG8	**1.08 ± 0.36**	**0.28 ± 0.04**	**0.04**	*0.70 ± 0.22*	*0.23 ± 0.05*	*0.08*
BECN1	**0.74 ± 0.08**	**0.52 ± 0.02**	**0.03**	0.68 ± 0.16	0.55 ± 0.10	0.53
LC3	**0.99 ± 0.17**	**0.52 ± 0.02**	**0.0498**	0.83 ± 0.09	0.74 ± 0.08	0.47
ULK1	**0.86 ± 0.12**	**0.38 ± 0.01**	**0.02**	**0.80 ± 0.13**	**0.40 ± 0.05**	**0.047**
GADD 45	1.49 ± 0.42	2.17 ± 0.35	0.28	0.27 ± 0.08	0.36 ± 0.07	0.45
SESN1	1.12 ± 0.28	1.23 ± 0.12	0.73	0.38 ± 0.12	0.51 ± 0.02	0.36
SESN2	0.88 ± 0.15	0.72 ± 0.02	0.37	0.43 ± 0.09	0.51 ± 0.03	0.42
SOD1	1.10 ± 0.10	1.33 ± 0.03	0.17	0.64 ± 0.06	0.67 ± 0.05	0.71
SOD2	1.07 ± 0.03	1.08 ± 0.12	0.95	0.97 ± 0.15	0.87 ± 0.10	0.62
CAT	0.52 ± 0.16	0.30 ± 0.02	0.22	0.18 ± 0.06	0.13 ± 0.02	0.42

Gene expression by qPCR in the heart of ApoE$^{-/-}$Timp3$^{-/-}$ and ApoE$^{-/-}$ mice in the fasting and fed state. Data are mean ± SEM (Bold indicates $p < 0.05$ and italics $0.05 < p < 0.1$, Student's t test, n = 4—5 per group).

Forkhead box protein O1 (FoxO1), which is involved in energy metabolism, but also in autophagy. Coupled with this, its targets ATG5, ATG8, BECN1 and LC3 were also downregulated in ApoE$^{-/-}$TIMP3$^{-/-}$ mice. Decreased autophagy has been related to heart failure and this reduction might contribute to the reduced heart function we observed in our model of post-ischemic heart failure [48].

The occurrence of cardiovascular mortality in ApoE$^{-/-}$TIMP3$^{-/-}$ mice might reflect a complex interaction between metabolic defects and tissue remodeling consequent to increased inflammation and tissue degeneration. Using whole heart mRNA sequencing and subsequent real-time PCR analysis we revealed apelin as a possible mediator of the metabolic effects by TIMP3. In ApoE$^{-/-}$TIMP3$^{-/-}$ mice, we found apelin to be decreased in the circulation as well as downregulated at the myocardial level compared to other sites of expression such as the adipose tissue [49]. Apelin supplementation restored impaired lipid oxidation in ApoE$^{-/-}$TIMP3$^{-/-}$ mice. Therefore, our data provide a molecular clue for the molecular phenotype observed in ApoE$^{-/-}$TIMP3$^{-/-}$ mice.

Apelin has recently been shown to rescue defects in insulin resistance and FAO possibly via regulation of AMPK signaling [27,49]. However, whether a long-term administration of Apelin is sufficient to prevent lipid accumulation and which signaling pathways contribute remains to be investigated.

The effect of TIMP3 on apelin might also explain decreased heart function in post-ischemic heart failure we observed in the ApoE$^{-/-}$TIMP3$^{-/-}$ mice. Patients with left ventricular systolic dysfunction exhibit decreased myocardial apelin expression in the left ventricular wall [50], and experimental in vivo data link apelin to positive inotropic and regenerative effects in both normal hearts and post-ischemic heart failure [51—54]. We did not test the effects of apelin on experimental myocardial infarction. However, it has previously been shown that in a rat model of post ischemic heart failure, also using the model of LAD ligation, apelin supplementation was able to reduce infarction size [55].

ApoE$^{-/-}$TIMP3$^{-/-}$ mice displayed an impaired oxidative stress response. Chronic treatment of mice with apelin attenuated pressure-overload-induced left ventricular hypertrophy, by increasing the oxidative stress response [56], and decreased ischemia/reperfusion injury by restoring levels of antioxidant defense [57]. Thus, reduced apelin levels found in the ApoE$^{-/-}$TIMP3$^{-/-}$ mice may also be responsible in part for other metabolomics findings of our study. Recently, it has been reported that apelin reduces sphingosine kinase 1 activity in cardiac fibroblasts [58] and might therefore increase levels of sphingosine.

Since reduced apelin levels have also been associated with arrhythmias [59,60], we hypothesize that reduced apelin may contribute to the pro-arrythmogenic phenotype that we observed in the ApoE$^{-/-}$TIMP3$^{-/-}$ model. However, a positive effect of apelin supplementation on arrhythmias in this model remains to be seen.

We have previously reported that loss of TIMP3 has a role in the pathogenesis obesity-associated non-alcoholic fatty liver disease (NAFLD) [8]. We did not measure the lipid content of the liver in this study, but the fact that the livers of ApoE$^{-/-}$TIMP3$^{-/-}$ mice reveal similar defects in the expression of PPARα and FoxO1 targets,

 © 2015 The Authors. Published by Elsevier GmbH. This is an open access article under the CC BY-NC-ND license (http://creativecommons.org/licenses/by-nc-nd/4.0/).

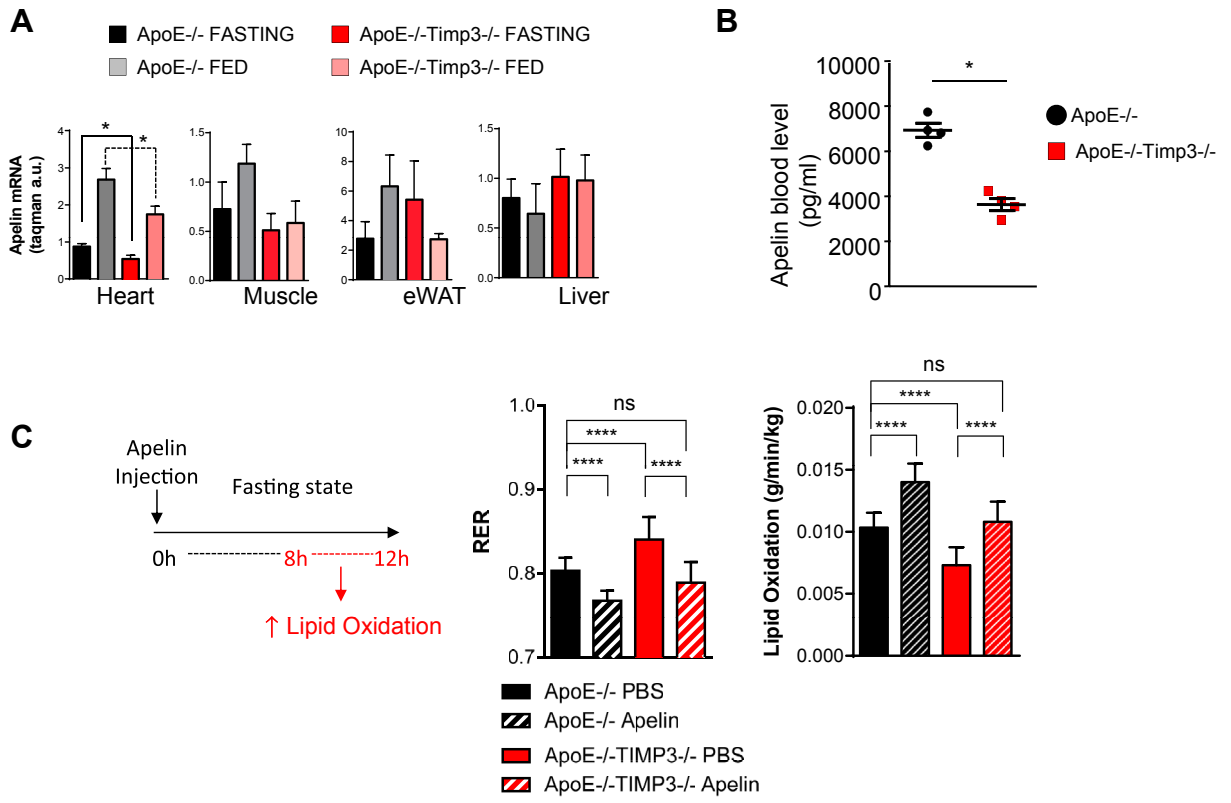

Figure 7: Loss of TIMP3 leads to disrupted apelin secretion from heart while supplementation can correct some of the metabolic abnormalities in the heart. A) Apelin expression by qPCR in heart, muscle, adipose tissue and liver reveals a difference between ApoE$^{-/-}$TIMP3$^{-/-}$ and ApoE$^{-/-}$ animals only in the heart (*$p < 0.05$, one-way ANOVA, $n = 5$ per group). B) Circulating apelin levels measured by ELISA were also found to be reduced in the ApoE$^{-/-}$TIMP3$^{-/-}$ (*$p < 0.05$, Student's t test, $n = 4$ per group). C) Single dose of intraperitoneally injected apelin restores impaired lipid oxidation of ApoE$^{-/-}$TIMP3$^{-/-}$ mice during the prolonged fasting state (interval of 8–12 h) measured by indirect calorimetry. Data are mean ± SEM (****$p < 0.001$, one-way ANOVA, $n = 5$–6 per group).

including SCD1, suggests that inter-organs crosstalk might be involved in the phenotype observed. Previous studies have shown that SCD1 deficiency is correlated to diet-induced fatty liver disease. NAFLD has also been linked to increased cardiovascular risk, myocardial remodeling and dysfunction as well as prolongation of QTc interval and thus increased risk of arrhythmias [61]. However, we did not observe alterations in hepatic apelin expression suggesting the involvement of different pathways. Overall, we cannot exclude that part of the phenotype is sustained by a liver to heart axis.

Interestingly, metabolomics analysis also revealed an alteration of gut micro biota-derived (host co-) metabolites such as serotonin, N-acetyltryptophan and 3-indoxyl sulfate in the ApoE$^{-/-}$TIMP3$^{-/-}$ (Supplementary Table 2). TIMP3 has been shown to regulate lymphocyte populations [62] as well as to mediate colonic epithelial barrier disruption through ADAM17 and might, therefore, be involved in shaping the gut microbiota and regulation of gut microbiota/host interactions, leading to altered immune and metabolic processes. Backhed and colleagues could show that germ-free mice exhibited altered gene expression of enzymes involved in fatty acid oxidation [63]. Therefore, an alteration of the gut microbiota might contribute to the phenotype observed in the ApoE$^{-/-}$TIMP3$^{-/-}$ mice.

5. CONCLUSION

TIMP3 maintains cardiac metabolic flexibility in conditions of increased stress such as myocardial infarction. Deficiency of TIMP3 results in perturbations of oxidative stress response, sphingolipid pathway and lipid metabolism. Reduced levels of apelin found in ApoE$^{-/-}$TIMP3$^{-/-}$ mice partly explain the defects, and supplementation of apelin rescues the metabolic phenotype by increasing lipid oxidation.

ACKNOWLEDGEMENTS

M.F. laboratory is funded by Fondazione Roma Grant 2008, Progetto SID 2013, FP-7 EURHYTHDIA (contract grant agreement no. 278397), FP7-FLORINASH (contract grant agreement no. 241913), PRIN 201223BJ89E and Associazione Italiana per la Ricerca sul Cancro (Grant AIRC IG-13163); A.C. is supported by FIRB RBAP10L8TY and Fondazione Roma. R.S. is supported by a grant from the Deutsche Herzstiftung (DHS) and a PhD fellowship from the University of Rome Tor Vergata. B.K. is supported by a PhD fellowship from the University of Rome Tor Vergata.

CONFLICT OF INTEREST

The authors have no conflict of interest to disclose regarding the content of this manuscript.

AUTHOR CONTRIBUTIONS

M.F. conceived the experimental plan; R.S., B.K., M.C., M.M., V.C. performed mouse and laboratory experiments and analyzed data; D.C., V.F., G.C., G.L., performed Telemetry and ECG analyses; A.C. and I.A analyzed the heart RNA sequencing data;

 © 2015 The Authors. Published by Elsevier GmbH. This is an open access article under the CC BY-NC-ND license (http://creativecommons.org/licenses/by-nc-nd/4.0/).

S.R. contributed to statistical analysis and the discussion; R.S, B.K., R.M. and M.F. wrote the manuscript.

APPENDIX A. SUPPLEMENTARY DATA

Supplementary data related to this article can be found at http://dx.doi.org/10.1016/j.molmet.2015.07.007.

REFERENCES

[1] Lopaschuk, G.D., Ussher, J.R., Folmes, C.D., Jaswal, J.S., Stanley, W.C., 2010. Myocardial fatty acid metabolism in health and disease. Physiological Reviews 90:207–258.

[2] Schafer, Z.T., Grassian, A.R., Song, L., Jiang, Z., Gerhart-Hines, Z., Irie, H.Y., et al., 2009. Antioxidant and oncogene rescue of metabolic defects caused by loss of matrix attachment. Nature 461:109–113.

[3] Spinale, F.G., Zile, M.R., 2013. Integrating the myocardial matrix into heart failure recognition and management. Circulation Research 113:725–738.

[4] Carnevale, D., Lembo, G., 2012. Placental growth factor and cardiac inflammation. Trends in Cardiovascular Medicine 22:209–212.

[5] Federici, M., Hribal, M.L., Menghini, R., Kanno, H., Marchetti, V., Porzio, O., et al., 2005. Timp3 deficiency in insulin receptor-haploinsufficient mice promotes diabetes and vascular inflammation via increased TNF-alpha. Journal of Clinical Investigation 115:3494–3505.

[6] Cardellini, M., Menghini, R., Martelli, E., Casagrande, V., Marino, A., Rizza, S., et al., 2009. TIMP3 is reduced in atherosclerotic plaques from subjects with type 2 diabetes and increased by SirT1. Diabetes 58:2396–2401.

[7] Menghini, R., Casagrande, V., Menini, S., Marino, A., Marzano, V., Hribal, M.L., et al., 2012. TIMP3 overexpression in macrophages protects from insulin resistance, adipose inflammation, and nonalcoholic fatty liver disease in mice. Diabetes 61:454–462.

[8] Menghini, R., Menini, S., Amoruso, R., Fiorentino, L., Casagrande, V., Marzano, V., et al., 2009. Tissue inhibitor of metalloproteinase 3 deficiency causes hepatic steatosis and adipose tissue inflammation in mice. Gastroenterology 136:663–672.

[9] Fiorentino, L., Cavalera, M., Menini, S., Marchetti, V., Mavilio, M., Fabrizi, M., et al., 2013. Loss of TIMP3 underlies diabetic nephropathy via FoxO1/STAT1 interplay. EMBO Molecular Medicine 5:441–455.

[10] Casagrande, V., Menghini, R., Menini, S., Marino, A., Marchetti, V., Cavalera, M., et al., 2012. Overexpression of tissue inhibitor of metalloproteinase 3 in macrophages reduces atherosclerosis in low-density lipoprotein receptor knockout mice. Arteriosclerosis Thrombosis and Vascular Biology 32:74–81.

[11] Monroy, A., Kamath, S., Chavez, A.O., Centonze, V.E., Veerasamy, M., Barrentine, A., et al., 2009. Impaired regulation of the TNF-alpha converting enzyme/tissue inhibitor of metalloproteinase 3 proteolytic system in skeletal muscle of obese type 2 diabetic patients: a new mechanism of insulin resistance in humans. Diabetologia 52:2169–2181.

[12] Khokha, R., Murthy, A., Weiss, A., 2013. Metalloproteinases and their natural inhibitors in inflammation and immunity. Nature Reviews Immunology 13:649–665.

[13] Basu, R., Lee, J., Morton, J.S., Takawale, A., Fan, D., Kandalam, V., et al., 2013. TIMP3 is the primary TIMP to regulate agonist-induced vascular remodelling and hypertension. Cardiovascular Research 98:360–371.

[14] Basu, R., Fan, D., Kandalam, V., Lee, J., Das, S.K., Wang, X., et al., 2012. Loss of Timp3 gene leads to abdominal aortic aneurysm formation in response to angiotensin II. Journal of Biological Chemistry 287:44083–44096.

[15] Kassiri, Z., Oudit, G.Y., Sanchez, O., Dawood, F., Mohammed, F.F., Nuttall, R.K., et al., 2005. Combination of tumor necrosis factor-alpha ablation and matrix metalloproteinase inhibition prevents heart failure after pressure overload in tissue inhibitor of metalloproteinase-3 knock-out mice. Circulation Research 97:380–390.

[16] Fedak, P.W., Smookler, D.S., Kassiri, Z., Ohno, N., Leco, K.J., Verma, S., et al., 2004. TIMP-3 deficiency leads to dilated cardiomyopathy. Circulation 110:2401–2409.

[17] Qi, J.H., Ebrahem, Q., Moore, N., Murphy, G., Claesson-Welsh, L., Bond, M., et al., 2003. A novel function for tissue inhibitor of metalloproteinases-3 (TIMP3): inhibition of angiogenesis by blockage of VEGF binding to VEGF receptor-2. Nature Medicine 9:407–415.

[18] Saunders, W.B., Bohnsack, B.L., Faske, J.B., Anthis, N.J., Bayless, K.J., Hirschi, K.K., et al., 2006. Coregulation of vascular tube stabilization by endothelial cell TIMP-2 and pericyte TIMP-3. Journal of Cell Biology 175:179–191.

[19] Kandalam, V., Basu, R., Abraham, T., Wang, X., Awad, A., Wang, W., et al., 2010. Early activation of matrix metalloproteinases underlies the exacerbated systolic and diastolic dysfunction in mice lacking TIMP3 following myocardial infarction. American Journal of Physiology. Heart and Circulatory Physiology 299:H1012–H1023.

[20] Tian, H., Cimini, M., Fedak, P.W., Altamentova, S., Fazel, S., Huang, M.L., et al., 2007. TIMP-3 deficiency accelerates cardiac remodeling after myocardial infarction. Journal of Molecular and Cellular Cardiology 43:733–743.

[21] Carnevale, D., Cifelli, G., Mascio, G., Madonna, M., Sbroggio, M., Perrino, C., et al., 2011. Placental growth factor regulates cardiac inflammation through the tissue inhibitor of metalloproteinases-3/tumor necrosis factor-alpha-converting enzyme axis: crucial role for adaptive cardiac remodeling during cardiac pressure overload. Circulation 124:1337–1350.

[22] Fedak, P.W., Altamentova, S.M., Weisel, R.D., Nili, N., Ohno, N., Verma, S., et al., 2003. Matrix remodeling in experimental and human heart failure: a possible regulatory role for TIMP-3. American Journal of Physiology. Heart and Circulatory Physiology 284:H626–H634.

[23] Fiorentino, L., Cavalera, M., Mavilio, M., Conserva, F., Menghini, R., Gesualdo, L., et al., 2013. Regulation of TIMP3 in diabetic nephropathy: a role for microRNAs. Acta Diabetologica 50:965–969.

[24] Stohr, R., Cavalera, M., Menini, S., Mavilio, M., Casagrande, V., Rossi, C., et al., 2014. Loss of TIMP3 exacerbates atherosclerosis in ApoE null mice. Atherosclerosis 235:438–443.

[25] Tarnavski, O., McMullen, J.R., Schinke, M., Nie, Q., Kong, S., Izumo, S., 2004. Mouse cardiac surgery: comprehensive techniques for the generation of mouse models of human diseases and their application for genomic studies. Physiological Genomics 16:349–360.

[26] Marino, A., Menghini, R., Fabrizi, M., Casagrande, V., Mavilio, M., Stoehr, R., et al., 2014. ITCH deficiency protects from diet-induced obesity. Diabetes 63:550–561.

[27] Attane, C., Foussal, C., Le Gonidec, S., Benani, A., Daviaud, D., Wanecq, E., et al., 2012. Apelin treatment increases complete fatty acid oxidation, mitochondrial oxidative capacity, and biogenesis in muscle of insulin-resistant mice. Diabetes 61:310–320.

[28] Saeed, A.I., Bhagabati, N.K., Braisted, J.C., Liang, W., Sharov, V., Howe, E.A., et al., 2006. TM4 microarray software suite. Methods in Enzymology 411:134–193.

[29] Braun, A., Trigatti, B.L., Post, M.J., Sato, K., Simons, M., Edelberg, J.M., et al., 2002. Loss of SR-BI expression leads to the early onset of occlusive atherosclerotic coronary artery disease, spontaneous myocardial infarctions, severe cardiac dysfunction, and premature death in apolipoprotein E-deficient mice. Circulation Research 90:270–276.

[30] Martin, K.R., 2010. The bioactive agent ergothioneine, a key component of dietary mushrooms, inhibits monocyte binding to endothelial cells characteristic of early cardiovascular disease. Journal of Medicinal Food 13:1340–1346.

[31] Nagarajan, S., Burris, R.L., Stewart, B.W., Wilkerson, J.E., Badger, T.M., 2008. Dietary soy protein isolate ameliorates atherosclerotic lesions in apolipoprotein E-deficient mice potentially by inhibiting monocyte chemoattractant protein-1 expression. Journal of Nutrition 138:332–337.

 © 2015 The Authors. Published by Elsevier GmbH. This is an open access article under the CC BY-NC-ND license (http://creativecommons.org/licenses/by-nc-nd/4.0/).

[32] Ko, Y.E., Lee, I.H., So, H.M., Kim, H.W., Kim, Y.H., 2011. Mechanism of glutathione depletion during simulated ischemia-reperfusion of H9c2 cardiac myocytes. Free Radical Research 45:1074–1082.
[33] Valbuena-Diez, A.C., Blanco, F.J., Oujo, B., Langa, C., Gonzalez-Nunez, M., Llano, E., et al., 2012. Oxysterol-induced soluble endoglin release and its involvement in hypertension. Circulation 126:2612–2624.
[34] Barth, J.L., Yu, Y., Song, W., Lu, K., Dashti, A., Huang, Y., et al., 2007. Oxidised, glycated LDL selectively influences tissue inhibitor of metalloproteinase-3 gene expression and protein production in human retinal capillary pericytes. Diabetologia 50:2200–2208.
[35] Hayter, H.L., Pettus, B.J., Ito, F., Obeid, L.M., Hannun, Y.A., 2001. TNFalpha-induced glutathione depletion lies downstream of cPLA(2) in L929 cells. FEBS Letters 507:151–156.
[36] Egom, E.E., Mamas, M.A., Chacko, S., Stringer, S.E., Charlton-Menys, V., El-Omar, M., et al., 2013. Serum sphingolipids level as a novel potential marker for early detection of human myocardial ischaemic injury. Frontiers in Physiology 4:130.
[37] Knapp, M., Zendzian-Piotrowska, M., Blachnio-Zabielska, A., Zabielski, P., Kurek, K., Gorski, J., 2012. Myocardial infarction differentially alters sphingolipid levels in plasma, erythrocytes and platelets of the rat. Basic Research in Cardiology 107:294.
[38] Cavalli, A.M.L.J., Gellings, N.M., Castro, E., Page, T.M., Klepper, R.E., Palade, P.T., et al., 2002. The role of TNFα and sphingolipid signaling in cardiac hypoxia: evidence that cardiomyocytes release TNFα and sphingosine. Basic and Applied Myology 12:167–175.
[39] Cordis, G.A., Yoshida, T., Das, D.K., 1998. HPTLC analysis of sphingomylein, ceramide and sphingosine in ischemic/reperfused rat heart. Journal of Pharmaceutical and Biomedical Analysis 16:1189–1193.
[40] Bai, Y., Wang, J., Shan, H., Lu, Y., Zhang, Y., Luo, X., et al., 2007. Sphingolipid metabolite ceramide causes metabolic perturbation contributing to HERG K+ channel dysfunction. Cellular Physiology and Biochemistry 20:429–440.
[41] Dobrzyn, P., Sampath, H., Dobrzyn, A., Miyazaki, M., Ntambi, J.M., 2008. Loss of stearoyl-CoA desaturase 1 inhibits fatty acid oxidation and increases glucose utilization in the heart. American Journal of Physiology. Endocrinology and Metabolism 294:E357–E364.
[42] Campbell, F.M., Kozak, R., Wagner, A., Altarejos, J.Y., Dyck, J.R., Belke, D.D., et al., 2002. A role for peroxisome proliferator-activated receptor alpha (PPARalpha) in the control of cardiac malonyl-CoA levels: reduced fatty acid oxidation rates and increased glucose oxidation rates in the hearts of mice lacking PPARalpha are associated with higher concentrations of malonyl-CoA and reduced expression of malonyl-CoA decarboxylase. Journal of Biological Chemistry 277:4098–4103.
[43] Kolwicz Jr., S.C., Tian, R., 2011. Glucose metabolism and cardiac hypertrophy. Cardiovascular Research 90:194–201.
[44] Sambandam, N., Morabito, D., Wagg, C., Finck, B.N., Kelly, D.P., Lopaschuk, G.D., 2006. Chronic activation of PPARalpha is detrimental to cardiac recovery after ischemia. American Journal of Physiology. Heart and Circulatory Physiology 290:H87–H95.
[45] Yue, T.L., Bao, W., Jucker, B.M., Gu, J.L., Romanic, A.M., Brown, P.J., et al., 2003. Activation of peroxisome proliferator-activated receptor-alpha protects the heart from ischemia/reperfusion injury. Circulation 108:2393–2399.
[46] Lou, P.H., Zhang, L., Lucchinetti, E., Heck, M., Affolter, A., Gandhi, M., et al., 2013. Infarct-remodelled hearts with limited oxidative capacity boost fatty acid oxidation after conditioning against ischaemia/reperfusion injury. Cardiovascular Research 97:251–261.
[47] Sena, S., Hu, P., Zhang, D., Wang, X., Wayment, B., Olsen, C., et al., 2009. Impaired insulin signaling accelerates cardiac mitochondrial dysfunction after myocardial infarction. Journal of Molecular and Cellular Cardiology 46:910–918.
[48] Ferdous, A., Battiprolu, P.K., Ni, Y.G., Rothermel, B.A., Hill, J.A., 2010. FoxO, autophagy, and cardiac remodeling. Journal of Cardiovascular Translational Research 3:355–364.
[49] Castan-Laurell, I., Dray, C., Knauf, C., Kunduzova, O., Valet, P., 2012. Apelin, a promising target for type 2 diabetes treatment? Trends in Endocrinology & Metabolism 23:234–241.
[50] Chandrasekaran, B., Kalra, P.R., Donovan, J., Hooper, J., Clague, J.R., McDonagh, T.A., 2010. Myocardial apelin production is reduced in humans with left ventricular systolic dysfunction. Journal of Cardiac Failure 16:556–561.
[51] Wang, W., McKinnie, S.M., Patel, V.B., Haddad, G., Wang, Z., Zhabyeyev, P., et al., 2013. Loss of apelin exacerbates myocardial infarction adverse remodeling and ischemia-reperfusion injury: therapeutic potential of synthetic apelin analogues. Journal of the American Heart Association 2:e000249.
[52] Scimia, M.C., Hurtado, C., Ray, S., Metzler, S., Wei, K., Wang, J., et al., 2012. APJ acts as a dual receptor in cardiac hypertrophy. Nature 488:394–398.
[53] Tempel, D., de Boer, M., van Deel, E.D., Haasdijk, R.A., Duncker, D.J., Cheng, C., et al., 2012. Apelin enhances cardiac neovascularization after myocardial infarction by recruiting aplnr+ circulating cells. Circulation Research 111:585–598.
[54] Li, L., Zeng, H., Chen, J.X., 2012. Apelin-13 increases myocardial progenitor cells and improves repair postmyocardial infarction. American Journal of Physiology. Heart and Circulatory Physiology 303:H605–H618.
[55] Azizi, Y., Faghihi, M., Imani, A., Roghani, M., Nazari, A., 2013. Post-infarct treatment with [Pyr1]-apelin-13 reduces myocardial damage through reduction of oxidative injury and nitric oxide enhancement in the rat model of myocardial infarction. Peptides 46:76–82.
[56] Foussal, C., Lairez, O., Calise, D., Pathak, A., Guilbeau-Frugier, C., Valet, P., et al., 2010. Activation of catalase by apelin prevents oxidative stress-linked cardiac hypertrophy. FEBS Letters 584:2363–2370.
[57] Pisarenko, O.I., Lankin, V.Z., Konovalova, G.G., Serebryakova, L.I., Shulzhenko, V.S., Timoshin, A.A., et al., 2014. Apelin-12 and its structural analog enhance antioxidant defense in experimental myocardial ischemia and reperfusion. Molecular and Cellular Biochemistry 391:241–250.
[58] Pchejetski, D., Foussal, C., Alfarano, C., Lairez, O., Calise, D., Guilbeau-Frugier, C., et al., 2012. Apelin prevents cardiac fibroblast activation and collagen production through inhibition of sphingosine kinase 1. European Heart Journal 33:2360–2369.
[59] Kallergis, E.M., Manios, E.G., Kanoupakis, E.M., Mavrakis, H.E., Goudis, C.A., Maliaraki, N.E., et al., 2010. Effect of sinus rhythm restoration after electrical cardioversion on apelin and brain natriuretic peptide prohormone levels in patients with persistent atrial fibrillation. American Journal of Cardiology 105:90–94.
[60] Ellinor, P.T., Low, A.F., Macrae, C.A., 2006. Reduced apelin levels in lone atrial fibrillation. European Heart Journal 27:222–226.
[61] Targher, G., Valbusa, F., Bonapace, S., Bertolini, L., Zenari, L., Pichiri, I., et al., 2014. Association of nonalcoholic fatty liver disease with QTc interval in patients with type 2 diabetes. Nutrition, Metabolism & Cardiovascular Diseases 24:663–669.
[62] Murthy, A., Shao, Y.W., Defamie, V., Wedeles, C., Smookler, D., Khokha, R., 2012. Stromal TIMP3 regulates liver lymphocyte populations and provides protection against Th1 T cell-driven autoimmune hepatitis. Journal of Immunology 188:2876–2883.
[63] Backhed, F., Manchester, J.K., Semenkovich, C.F., Gordon, J.I., 2007. Mechanisms underlying the resistance to diet-induced obesity in germ-free mice. Proceedings of the National Academy of Sciences of the United States of America 104:979–984.

 © 2015 The Authors. Published by Elsevier GmbH. This is an open access article under the CC BY-NC-ND license (http://creativecommons.org/licenses/by-nc-nd/4.0/).